Title
Atomic force microscopy investigation of the giant mimivirus.

Journal
Virology, 404(1)

ISSN
0042-6822

Authors
Kuznetsov, Yuri G
Xiao, Chuan
Sun, Siyang
et al.

Publication Date
2010-08-01

DOI
10.1016/j.virol.2010.05.007

Virology 404 (2010) 127–137

Contents lists available at ScienceDirect

Virology

journal homepage: www.elsevier.com/locate/yviro

Atomic force microscopy investigation of the giant mimivirus

Yuri G. Kuznetsov [a], Chuan Xiao [b], Siyang Sun [c], Didier Raoult [d], Michael Rossmann [c], Alexander McPherson [a,*]

[a] Department of Molecular Biology and Biochemistry, University of California, Irvine, CA 92697-3900, USA
[b] Department of Chemistry, University of El Paso, El Paso, TX, USA
[c] Department of Biological Science, Purdue University, West Lafayette, IN 47907, USA
[d] Unite des Rickettsies Faculte de Medecine, (CNRS), UMR 6020, IFR 48, Marseille, France

ARTICLE INFO

Article history:
Received 30 March 2010
Accepted 5 May 2010

Keywords:
AFM
Structure
Stargate
Icosahedron
Membrane
DNA

ABSTRACT

Mimivirus was investigated by atomic force microscopy in its native state following serial degradation by lysozyme and bromelain. The 750-nm diameter virus is coated with a forest of glycosylated protein fibers of lengths about 140 nm with diameters 1.4 nm. Fibers are capped with distinctive ellipsoidal protein heads of estimated Mr = 25 kDa. The surface fibers are attached to the particle through a layer of protein covering the capsid, which is in turn composed of the major capsid protein (MCP). The latter is organized as an open network of hexagonal rings with central depressions separated by 14 nm. The virion exhibits an elaborate apparatus at a unique vertex, visible as a star shaped depression on native particles, but on defibered virions as five arms of 50 nm width and 250 nm length rising above the capsid by 20 nm. The apparatus is integrated into the capsid and not applied atop the icosahedral lattice.

Prior to DNA release, the arms of the star disengage from the virion and it opens by folding back five adjacent triangular faces. A membrane sac containing the DNA emerges from the capsid in preparation for fusion with a membrane of the host cell. Also observed from disrupted virions were masses of distinctive fibers of diameter about 1 nm, and having a 7-nm periodicity. These are probably contained within the capsid along with the DNA bearing sac. The fibers were occasionally observed associated with toroidal protein clusters interpreted as processive enzymes modifying the fibers.

Introduction

Mimivirus (*Acanthamoeba polyphaga mimivirus*) warrants special attention owing to its size, complexity, and its evolutionary ambiguity. It is the largest virus known, having a diameter of 700 to 750 nm based on electron microscopy (Xiao et al., 2005; 2009; Zauberman et al., 2008) and a genome size of 1.2 million base pairs (Raoult et al., 2004), nearly twice that of any other known virus. Its linear, double-stranded DNA codes for 911 genes, and among these are many that are not expressed by any other virus, but only by living cells. The products include, for example tRNA synthetases, and enzymes for amino acid, carbohydrate, and lipid metabolism (Claverie et al., 2006; Raoult and Forterre, 2008).

Although there is some evidence that mimivirus can be associated with human pneumonia (Raoult et al., 2004; 2007), it is the focus of particular interest because its genomic, metabolic, and structural intricacy suggest that it might provide an evolutionary bridge between viruses and living cells (Benson et al., 2004; Claverie et al., 2006; Raoult and Forterre, 2008; Suzan-Monti et al., 2006). The virions contain membrane structures and complicated assemblies having specialized functions as in simple cells (Claverie et al., 2009; Forterre, 2006; Moreira and Lopez-Garcia, 2009).

The virus enters a host cell, an amoeba, by mimicry of a bacterial cell surface (Claverie et al., 2006; Raoult et al., 2004; Xiao et al., 2009). It is phagocytosed, its DNA delivered to the host cell, and there it is replicated and packaged inside an icosahedral capsid (Xiao et al., 2009). At a later stage, a forest of long, glycosylated fibers are added to the immature virion (Suzan-Monti et al., 2007). About 8 h following infection, the virus inside the cell reaches a critical mass, and the host cell bursts to release the daughter virions (Suzan-Monti et al., 2006).

Mimivirus appears most closely related structurally to large algal viruses such as PBCV-1 and other irridoviruses (Lyer et al., 2001; Van Etten et al., 1991; Yamada et al., 2006) though it possesses additional features not present in those viruses. Two recent studies by Zauberman et al. (2008) and Xiao et al. (2009) have added much detail to the current model of the structure of Mimivirus. The former investigation was based on cryoelectron transmission microscopy and electron tomography, and the later based on cryoelectron microscopy reconstruction, atomic force

* Corresponding author. Department of Molecular Biology & Biochemistry, University of California, Irvine, 560 Steinhaus Hall, Irvine, CA 92697-3900, USA. Fax: +1 949 824 8551.
E-mail address: amcphers@uci.edu (A. McPherson).

0042-6822/$ – see front matter © 2010 Elsevier Inc. All rights reserved.
doi:10.1016/j.virol.2010.05.007

microscopy (AFM), with some contribution from X-ray crystallography. While it is not reasonable to review all of the findings, some results are pertinent to the analysis presented here, which is based exclusively on AFM.

The work of Xiao (Xiao et al., 2009) revealed details of the icosahedral capsid, which consists of 20 large triangular plates joined at their edges to produce the required 12 fivefold vertices. The capsid surface is composed of trimeric major capsid proteins (MCP), each subunit of which consists of two jelly roll beta barrels, arranged in a very open hexagonal lattice, with the appearance of a honeycomb. The center-to-center distance of the capsomeres is 14 nm. Because there is some ambiguity as to what lies exactly on the fivefold vertex, there is an uncertainty in the triangulation number T, which could have any one of nine possibilities lying between 972 and 1200.

The fibers that coat particles are reported to have lengths of about 125 nm and are probably anchored to the MCPs or perhaps to an integument layer of protein disposed immediately above the capsid. The most striking and unique feature of mimivirus is a prominent five armed, star-shaped apparatus that occupies one vertex of every virus. While somewhat obscured on the intact virus, it is prominently displayed on particles which lack the coating of fibers. As Zauberman et al. (2008) have shown, this star shaped assembly, which they termed a "stargate," opens up, once the virus is inside the host cell, to produce a wide opening. The DNA of the virus, which is enclosed inside a membrane sac, then emerges from the interior, fuses with a cellular membrane, and delivers its nucleic acid contents to the cell. Another remarkable feature suggested by Zauberman et al. (2008), is that the DNA does not enter the capsid through the stargate, but through a separate portal, and by a completely different mechanism, in the center of a distal icosahedral face, i.e., at a threefold axis.

From the images recorded in our AFM investigation of mimivirus, we have visualized additional features of the fibers that cover the particles, the structure of the capsid, the membrane sac containing the DNA, and the DNA itself. We also describe the presence of a large quantity of unusual, long fibers having a distinctive 7 nm repeat that appear often upon disruption of viral capsids. From these observations, and those of earlier investigators, we have extended the structural model for mimivirus and have added new details.

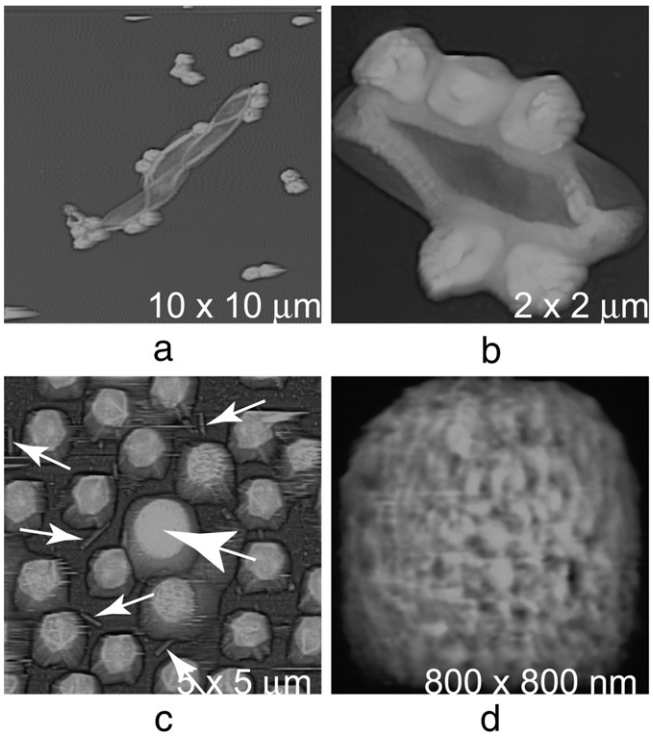

Fig. 1. In (a) is a low magnification AFM image of mimivirus that remain attached to a large fragment of membrane, presumably from the host amoeba. In (b) is a higher magnification image of virus clinging to membrane fragments. Extensive treatment with lysozyme and bromelain degraded virtually all mimivirus particles to capsids. In (c) in the center of the field (large arrow), however, is a full-sized, completely intact virus particle that, unlike its cohort, was enzyme resistant. In (d) is a higher magnification image of the same particle showing it to be typical of native mimivirus coated with surface fibers. Note in (c) the short rods scattered about in the background (small arrows). These have dimensions the same as the arms of the stargates, presumably lost intact when the stargates open.

Results

The strategy we pursued in dissecting mimivirus, seen attached to host cell membrane in Figs. 1a and b, was essentially the same as was employed in the dissection of vaccinia virus (Kuznetsov et al., 2008), a combination of chemical, enzymatic, and physical procedures designed to strip away successive layers of structure to reveal the one below. Of particular importance in this regard was the treatment of mimivirus with lysozyme followed by exposure to bromelain, and, in some cases, further exposure to proteinase K (Xiao et al., 2009). The virus is completely coated with a dense layer of protein fibers that are extensively glycosylated. The oligosaccharides, among other things, probably protect the protein fibers from proteolytic attack. Once the oligosaccharide linkages are degraded, at least in part, then the protein fibers are rendered susceptible to detachment by proteases. Serial treatment with the two enzymes proved essential to the exposure, for AFM analysis, of the capsid and its contents.

Upon treatment of native mimivirus with enzymes, virtually all particles were degraded to naked capsids. About 5% of the particles, however, were resistant to the enzymes and remained unscathed. One such virion is seen in Fig. 1c among a defibered cohort and in Fig. 1d at higher magnification. It remained coated with surface fibers, and exhibits a native diameter of 750 nm. Below we describe the internal organization of such a particle, as recorded by AFM, as successive layers of structure were removed, proceeding toward the interior of the capsid, and to the genomic DNA inside.

The surface fibers and protein head groups

When native particles were treated with lysozyme and bromelain, most fibers were simply shorn from the underlying surface and were no longer attached at the interior end to their capsid anchors. Defibered virus particles and vast quantities of individual fibers appeared on the AFM substrate. The attachment site to the capsid appears most susceptible to cleavage, as fibers generally seem to be of common length, and full length. Short fibers and free protein head groups were less commonly observed.

Fig. 2a through d present AFM images of fibers detached from the virus, though in a few cases still attached to anchoring polypeptide. Although individual fibers are generally seen apart from neighbors, it is not uncommon to see them emerge in clusters or tufts from bits and pieces of the underlying basal protein that anchors the fibers, like hairs from a scalp. Examples are seen in Fig. 2e and f. It appears that one anchor protein or one capsomere may be able to support the attachment of multiple surface fibers. This is suggested both by direct observation of the clusters, and the fact that the surface fibers appear to be present in more copies than is the anchor (see below).

In AFM images of surface fibers that are free of anchoring protein and isolated on the substrate, as are those in Fig. 2a through d, the shafts of the fibers range in length from about 60 nm in a few cases up to about 140 nm for most. These fibers were produced, however, by treatment with lysozyme and bromelain, thus the fibers shorter than the maximum length are likely a consequence of proteolytic cleavage of the shafts. Heads are largely present on most of the surface fibers, however, indicating that attachment of the head protein is more

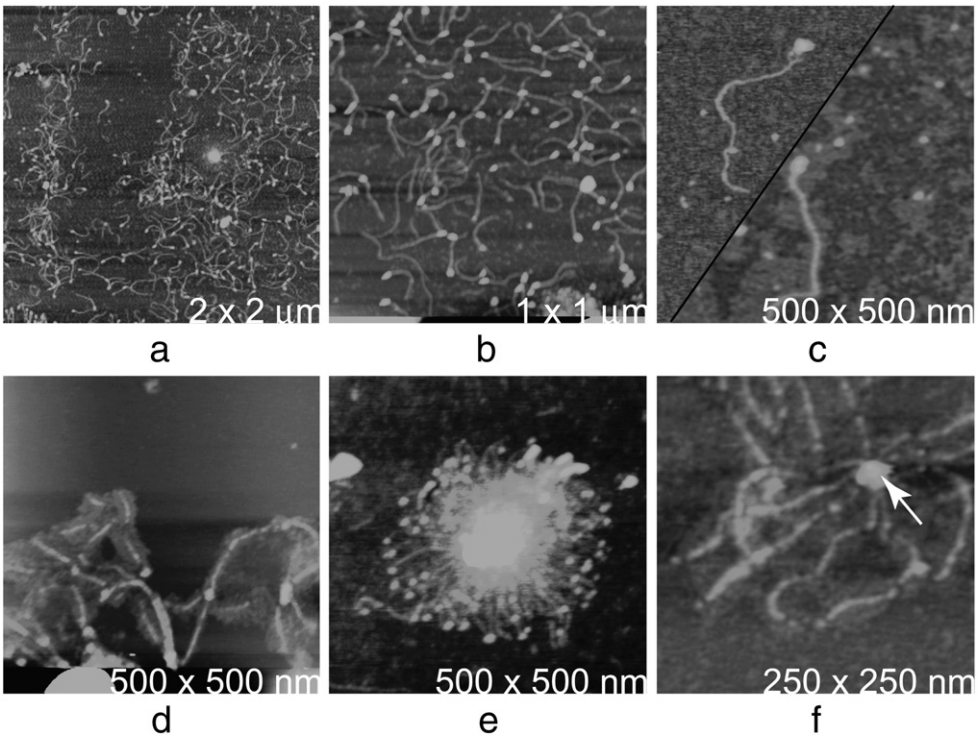

Fig. 2. In (a) is a mass of surface fibers, most still attached to their head groups, shed by mimivirus following treatment with lysozyme and bromelain. A cluster of fibers still attached to anchoring polypeptide at their proximal ends is also seen. In (b) the surface fibers are seen at higher magnification. The fibers are distinctive due to their more or less uniform lengths and the ellipsoidal protein heads. In (c) are two individual fibers, one of which is surrounded by a penumbra of some other material, and the shadows are even more prominent in other images, such as (d) where the coatings are quite pronounced. Presumably these are oligosaccharides that coat the shafts of the fibers. Surface fibers seen in (a) through (d) were completely detached from the particles by enzyme treatment. In (e) and (f) are fiber "crabs" where the surface fibers remain attached to clusters of the anchoring polypeptides or proteins that fix them in turn to the capsomeres. The cluster in (e) is large, but that in (f), marked with an arrow, probably represents only a few molecules of the anchoring protein.

resistant to protease attack than is the shaft or the connection to the underlying anchor polypeptide. The fibers appear structurally sound even with the persistence of proteolytic enzymes that might otherwise degrade them.

In those cases where we observed clusters of fibers still attached to underlying protein, as they are in Fig. 2e and f, the lengths of the surface fibers are uniform at about 130 to 140 nm with a diameter of about 1.4 nm. The absence of any appreciable variation in length suggests that the surface fiber shafts are either precisely "cut to measure" from longer precursor fibers, or that they are assembled from small precursors until the linear aggregate reaches some predetermined length.

It is known from other studies (Suzan-Monti et al., 2007; Zauberman et al., 2008) that the fibers are fabricated independent of the virus particles and attached later to "immature" particles. The "immature" particles, as we show below, have a layer of fiber anchoring polypeptide over their capsids. Thus the surface fibers do not grow from the surface of an immature particle like hairs from a scalp, nor are they first attached to an anchor protein and then the coiffed protein attached to the capsid.

In Fig. 2c two isolated fibers are seen displayed on the substrate, and they are reasonably representative of all of the fibers. One fiber is surrounded along its length by a shadow of material which rises only about half a nanometer above the substrate that is likely to be covalently attached oligosaccharide branching from the fiber shaft. The variation in the quantity associated with individual fibers is probably a function of their exposure to lysozyme, or due to differing extents of glycosylation by enzymes when the fibers are assembled. The coating of oligosaccharide is dense and likely explains the bacterial cell surface mimicry as well as the resistance of the fibers to degradation by proteases alone. It has been suggested that the fibers might be composed of collagen (Raoult et al., 2004; Xiao et al., 2005), but the absence of the appropriate periodicity and our finding that the fibers cannot be degraded by collagenase weighs against that proposal.

From 50 measurements of the heights of the distinctive protein heads that crown each of the surface fibers, and allowing for about 20% shrinkage due to dehydration, we estimate that the ellipsoidal shapes have minor axes **a** and **b** of about 3.5 nm and a major **c** axis of about 5 nm. The volume of an ellipsoid with those dimensions would be $4\pi/3\times(\mathbf{a}\times\mathbf{b}\times\mathbf{c})=28{,}870\ \mathrm{A}^3$. Comparison of this volume to that found for most proteins (McPherson, 1999) suggests a molecular weight of approximately 25 kDa. The head groups are likely responsible for the attachment of the virus to the surface of the amoeba. The protein heads occasionally detach from the tips of the fibers and can be seen on the substrate in the neighborhoods of fibers.

Surface fiber anchor layer

Between the base of a surface fiber and the MCP is a layer of material that connects the fibers to the capsid lattice. In Fig. 3a and b are AFM images of viral particles that have been incompletely degraded by lysozyme and bromelain. Some areas of the capsid lattice are exposed, but other areas still have anchoring material attached to the icosahedral shell, and often this continues to project surface fibers. The fibers can be resolved in these AFM scans because they lie against the capsid surface and assume stable orientations, and they are fixed there by exposure to glutaraldehyde. The AFM images do not indicate any additional lipid membrane or protein layer between the fibers and the icosahedral shell.

As illustrated by Fig. 3c in imaging native virus we occasionally encountered particles that completely lacked any fibers, while surrounded by particles that were covered by fibers. Presumably, these are immature virions, as it is known that preparations of virus

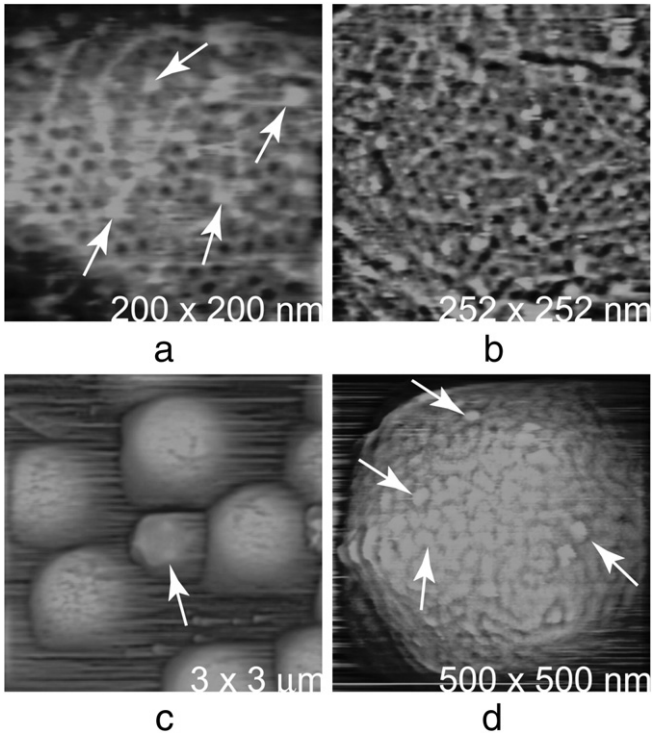

Fig. 3. In (a) and (b) are AFM images of mimivirus particles incompletely degraded with lysozyme and bromelain. Residual fibers are still connected to the icosahedral capsid, whose lattice is seen in patches in the background along with fragments of the anchoring protein (arrows). Among a population of native, untreated mimivirus, we occasionally observe small particles lacking any surface fibers as in (c) where it is marked with an arrow. Presumably these are immature particles on which the vertices of the icosahedron are obscured, but recognizable. In (d), the fiberless particle is seen at higher magnification. The capsid lattice is not evident, but the coating of fiber anchoring protein, some discrete units of which are marked with arrows, serves to connect the bases of the fiber shafts to the capsid protein (MCP) below.

normally contain some proportion of immature particles, and that the surface fibers are added to immature particles at a later stage (Suzan-Monti et al., 2007; Zauberman et al., 2008). The experimental value of these particles is that they allowed us to visualize the surface of the icosahedral capsid without being obscured by the fibers. In Fig. 3d, the layer of anchor material is seen as a more or less regular, closely packed array of protein units exhibiting similar sizes, suggesting that they are likely to have a common structure. The proteins protrude above the capsid surface by about 3 to 4 nm.

Although the layer of anchoring protein lacks the geometrical order of the underlying capsid network, at least in our AFM images, when discreet proteins are observed on the capsid surface, they appear to reside in the depressions of the capsid mesh. Thus whatever occupies the hexagonal indentations likely corresponds to the fiber anchors. There are about 3000 such depressions on the surface of the capsid, and we would expect there to be about the same number of fiber anchors. Unfortunately, we can make no good estimate of the density of surface fibers on a particle, thus we cannot determine the average number of surface fibers bound per depression. All we can say is that every anchor appears to provide multiple fiber binding sites.

The anchor protein may be an independent gene product layered atop the lattice of MCP, as some AFM images suggest. Alternately, the anchor protein layer may be composed of large, extended polypeptide loops of the MCP that protrude above the surface of the capsid. Indeed, the MCP has a "double jelly roll" structure with large external insertions between strands D and E (Xiao et al., 2009). If the loops were inclined toward the centers of the depressions in the lattice and coalesced there, then the appearance of such an aggregate would be equally consistent with the AFM images, such as that in Fig. 3d. This possibility is attractive because it could explain the multivalent fiber binding capacity of the anchor sites, and the high susceptibility of the anchor–fiber linkage to proteolysis.

The icosahedral capsid

The capsid of mimivirus, by virtue of its icosahedral symmetry (pseudo icosahedral if the "stargate" is considered), has been most amenable to visualization and analysis by cryo electron microscopy. Indeed its detailed architecture has recently been described, and even the arrangement of its major capsid protein on the icosahedral faces specified (Xiao et al., 2005, 2009; Zauberman et al., 2008). An advantage of AFM, however, is that it permits examination of individual particles and their singular features, including their defects. This has been done in the past on a variety of icosahedrally symmetric viruses that include BMV (Lucas et al., 2001), Mason–Pfizer monkey virus (Kuznetsov et al., 2007), Ty3 retrotransposon (Kuznetsov et al., 2005b) and the algal virus PBCV-1 (Kuznetsov et al., 2005a) for examples.

In the case of mimivirus, the open network of MCP, seen in Fig. 4, and having the honeycomb appearance of alternating hexagonal rings and depressions, became evident once external fibers were removed. The depressions in the network were accounted for by the absence of capsid proteins at these locations (Xiao et al., 2009).

In some high magnification images, such as those in Fig. 4a through c, and in Fourier filtered AFM images, as in Fig. 4d, the capsid network can be resolved into individual protein units arranged hexagonally around the perimeters of the depressions. Although the pattern is consistent with *p*3 plane group symmetry, if the depression contained an MCP, then the pattern would have *p*6 symmetry as expected (Xiao et al., 2009). We examined many images in an attempt to resolve with certainty what lay exactly on five-fold vertices, but were unable to do so.

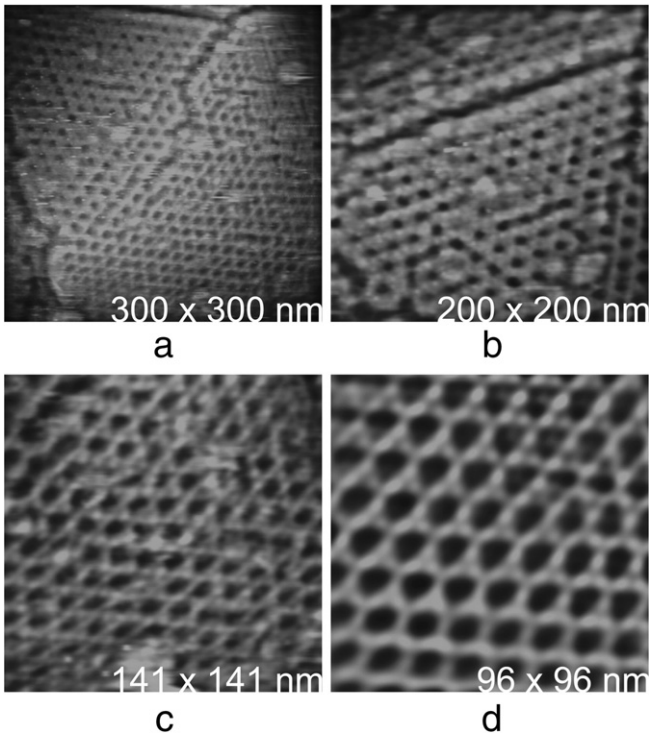

Fig. 4. When mimivirus has been exhaustively degraded with lysozyme, bromelain, and proteinase K, the protein lattice of the icosahedral shell becomes completely exposed. In (a), (b) and (c) are areas of the lattice. The distance between centers of the holes in the honeycomb network is 14 nm. There are numerous defects and scars on the capsids as a consequence of proteolysis. In (d) is a Fourier filtered image of the lattice seen in (c). In some areas, individual capsid proteins can be seen forming the hexameric rings.

The "Stargate" assembly

Perhaps the most striking and unique feature of mimivirus is a star-shaped area that occupies a fivefold vertex of each virion. As shown by Zauberman et al. (2008), the star shaped apparatus, which they appropriately named a "stargate," plays an important role in the delivery of genomic DNA. The "stargate" is in some ways functionally homologous to the tails of many bacteriophages as both are required for genome delivery. However there are important differences arising from the large genome size of the mimivirus and the mechanism of nucleic acid delivery.

The stargate apparatus, as illustrated by the AFM images in Fig. 5, is the most prominent feature on both intact particles and naked capsids. Each virion has one fivefold vertex committed to the stargate, and only one. Consistent with the observation of Zauberman et al. (2008) the apparatus is not coated with a layer of anchoring protein and, therefore, is not coated with fibers. As a consequence, the star lies substantially below the level of the fiber heads and is readily visualized by AFM as a star-shaped depression on the surfaces of intact particles.

On particles degraded by protease, additional details of the structure of the star apparatus emerge. The five arms of the star are about 50 nm in width as measured on fully hydrated particles. The arms extend almost to the next nearest vertices, as shown in Fig. 5f, but do not quite reach a vertex itself. The tips of the arms are somewhat rounded where they approach a vertex. Their length is about 250 nm. The arms protrude above the surface of the capsid by approximately 20 nm. They do not lie atop the capsid surface, that is, there is no capsid protein network beneath the arms. The arms are integrated into the capsid network. There is structural continuity between the arms and the surrounding icosahedral network of MCP. Nevertheless, when cracks appear along the edges of the arms and they begin to pull free of the surface, the cracks are always between the arm protein and the MCP array, indicating the junction of the two assemblies to be the line of least structural strength. In fully hydrated species, the arms appear to be monolithic for the most part.

We examined the centers of numerous stars to determine whether there was evidence of a hole, or if a plug existed at the center. We found both. In some cases there was the initiation of an opening, and in other cases the center was firmly blocked by a protein mass. The arms, in our AFM images, appeared as almost unitary entities, in that we saw comparatively little substructure on their surfaces. This was not due to poor resolution of the AFM images themselves, as often, the icosahedral network of the MCP was clearly resolved on either side of the star arms (Fig. 5c through f). This suggested to us that the arms might be composed of long fibers running their lengths. Nevertheless, we also observed that some stars on air dried samples had fractured arms with relatively well-defined transverse breaks. This would be unlikely if bundles or cables of fibers ran lengthwise.

It is noteworthy that while the fiber attachment site may be partly degraded by exposure to proteases, the arms of the stargate, which are completely unprotected by glycosylated fibers, seem to suffer no visible damage. Thus, whatever their composition, the stargate is surprisingly resistant to attack by cysteine and serine proteases.

The intact virus appears to shed the star assemblies prior to release of DNA. This is accomplished not by losing the star assembly as an integral unit, or by dissolution of the stars, but by casting off individual, intact arms of the star. In fact, free star arms can sometimes be found on the AFM substrate among native particles. Some of these were seen in Fig. 1c for example. Such a mechanism is also supported by images of particles in which the stargate has opened.

With the exception of the vertex exhibiting the star shaped apparatus, none of the other fivefold vertexes exhibit any prominent

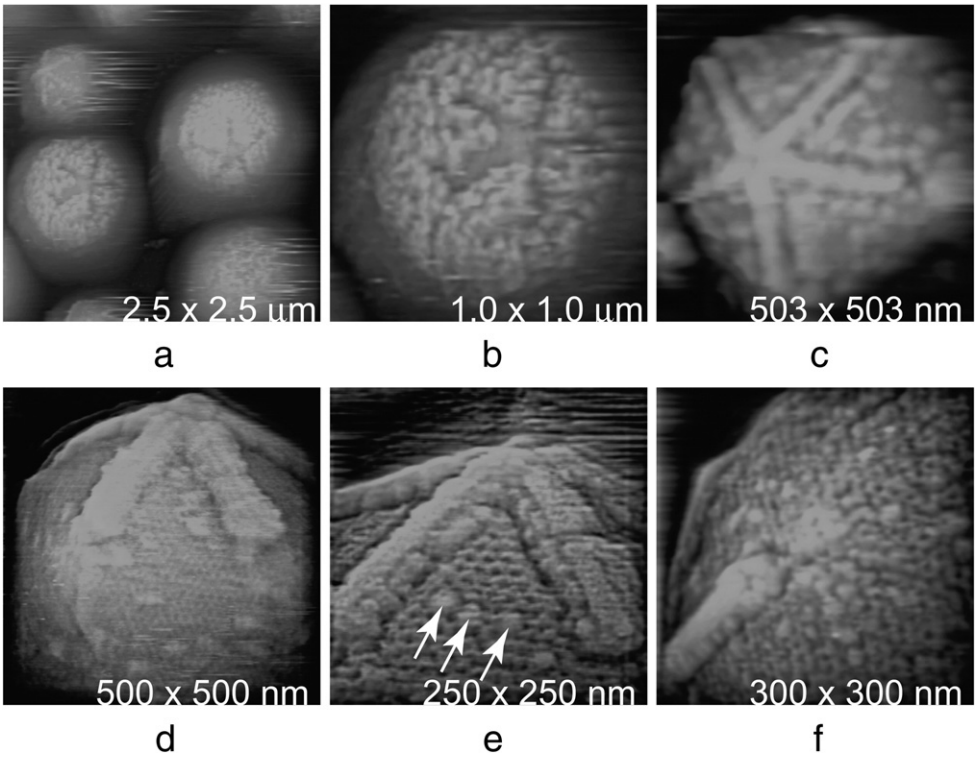

Fig. 5. In (a) and (b) are native mimivirus covered over almost their entire area by surface fibers. At one vertex on each particle, however, is a distinctive star shaped depression where the surface beneath is uncovered by the fibers. If the fibers and the underlying anchoring material is degraded by lysozyme and bromelain, then the star-shaped apparatus seen in (c), termed a "stargate" is revealed. The particle in (c) has not been completely degraded and portions of what may be the anchoring protein are still seen on the surface of the capsid. The arms of the stargate are coincident with icosahedral edges and are embedded in the capsid protein matrix. They are not coated with fibers. In (d) and (e) are higher magnification AFM images of the stargates showing their rise above the capsid surface, whose distinctive lattice is clearly evident over the remainder of the particles. Some anchor protein, or polypeptide clusters (marked with arrows) remain and can be seen on the surface just beneath the star in (e). The star appears to have a spine along its length and a more variegated border where it joins the capsid lattice. In (f) is an arm of a star that terminates just before reaching a neighboring fivefold vertex.

structure or unusual feature. This was not true in the study of the algal virus PBCV-1 (Kuznetsov et al., 2005a). In that virus, each vertex was marked by an aggregate of proteins that were distinctly different than the major capsid protein. In addition, there was at the center, lying exactly on the fivefold axis, a single, unique protein. This also was not seen in mimivirus.

Stargate opening and emergence of the DNA

One of the most striking electron micrographic images presented by Zauberman et al. (2008) was their Fig. 5b, that of a particle with the stargate open and five triangular faces folded out to reveal the membrane sac containing the DNA about to emerge. We recorded comparable images using AFM of stargates open, and in the process of opening. In Fig. 6a and b intact (not enzymatically treated) virus are shown at moderate and high magnification as the stargate begins to open. In Fig. 6a there are even intimations of the membrane sac behind the five triangular faces that make up the apparatus. The opening of the stargate can be seen in greater detail when enzymatically treated particles, including naked capsids begin to open as in Fig. 6c and d. In these images it is evident that the arms of the star have been lost entirely leaving behind an irregular ridge of material where the arms were joined to the capsid.

AFM images in Fig. 7 illustrate the consequence of the full opening of the stargate, that is, when the five triangular faces of the icosahedron that support the stargate have fully folded back. The interior sac, which is of lipid bilayer construction, derived presumably from a membrane of the previous host cell, and that contains the viral DNA, emerges from the capsid. In Fig. 7a and b are AFM scans of the capsid and the sac. The resolution of the images is confirmed by the capsid lattice where the honeycomb arrangement of capsomeres persists. It is clear from these images that delivery of the nucleic acid is totally different than for tailed phages where the DNA passes through a tube, or even for other large viruses such as PBCV-1 that lack such a stargate apparatus. This event, captured in Fig. 7, is clearly not unique, as there are empty capsids above and below it in Fig. 7a and other particles in Fig. 7c and d that have already lost their membrane sacs. The ultimate diameter of the aperture created for the emergence of the DNA containing sac appears to be significantly greater than the diameter of the sac itself. We estimate it to be 400 nm or more across.

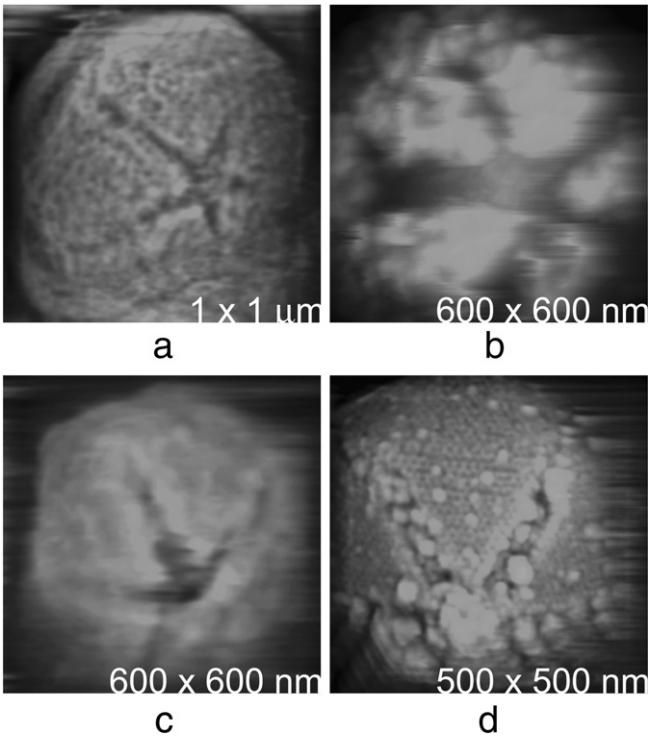

Fig. 6. In (a) and at higher magnification in (b) the stargate on a native undegraded mimivirus, now a five jawed aperture, is observed as it opens in preparation for release of the DNA. In (c) and (d) the opening of the jaws is more readily visualized on degraded particles where the naked capsid can be seen to draw back the five triangular faces of the icosahedron. As is evident here, the arms of the stars do not remain with the capsid but disengage entirely from the particles and are lost. Arms produced by this chain of events can be seen in the background in Fig. 1.

The diameter of the DNA sac, estimated from measurement on the AFM images, is about 340 nm, which would imply a spherical volume of approximately 2.1×10^7 nm^3. The amount of DNA contained in the sac is about 1.2×10^6 bp (Raoult et al., 2004), which gives a packing density of 0.06 nm^3/bp. This is almost the same as the packing density we estimated for the nucleic acid in the sac containing the DNA in vaccinia virus (Kuznetsov et al., 2008). It is more than ten times less than the packing density of DNA in the heads of bacteriophages lambda (Kindt et al., 2001) and P22 (Casjens and Weigele, 2005). The DNA in those two bacteriophages is known not to be associated with protein but to be packed with a density comparable to that observed in crystals of DNA (Casjens, 1997). Thus it may be concluded that the density of DNA in the mimivirus sac is relatively low and allows ample space for the accommodation of bound protein, as in vaccinia virus (Kuznetsov et al., 2008). This is consistent with AFM images that show the mimivirus DNA, within the capsid, to be extensively associated with large numbers of protein molecules (see below).

As noted above, the volume of the mimivirus sac containing its DNA is about 2.1×10^7 nm^3. The interior volume of an icosahedron is $2.18\times L^3$, where L is the edge length of the polygon. If we assume an edge length for the icosahedral capsid of 250 nm, which is in agreement with measurements from both EM and AFM, then the interior volume is approximately 3.4×10^7 nm^3. This implies that only about 65% of the interior volume of the icosahedral capsid is occupied by the DNA, its associated proteins, and the membrane sac in which they are contained. This further implies that there is a substantial space between the membrane sac and the interior walls of the icosahedral capsid. It is consistent, as well, with results from electron microscopy studies that show there to be a gap of from 30 nm to 50 nm between the membrane sac and the inside surface of the capsid (Xiao et al., 2009). Presumably, this extra interior space is filled with additional material, either produced exclusively by the virus to fill this space, or simply acquired by scooping up local material from the viral production site in the host amoeba (Suzan-Monti et al., 2007).

Empty capsids, like those in Fig. 7c and d, expose the insides of the triangular faces of the shells to the AFM tip, and thereby allow scanning of the inside surface of the capsid. As seen in Fig. 7e and f, the interior capsid surface is distinctly different than the outer surface of the capsid, which displays the highly geometric, icosahedral arrangement of MCP. The internal surface of the capsid appears to be coated with either a near continuous layer of proteins, or a lipid membrane with associated protein molecules. Indeed, a second lipid membrane has been suggested to exist between the sac containing the DNA and the inside capsid surface (Zauberman et al., 2008). In either case, this surface exhibits no regular, geometric pattern as is seen on the exterior.

The viral DNA

In spite of numerous attempts using chemical, physical, and enzymatic approaches, and in spite of the fact that some virus did so spontaneously, we could find only one means of inducing virus or degraded particles to release their DNA. Though lacking in elegance, the one sure way was mechanical pressure obtained by pressing particles between two sheets of atomically smooth, cleaved mica. DNA was produced in this way from some virions, as illustrated by Fig. 8, but many defibered particles in our samples apparently did not contain DNA at all. Possibly they had lost the nucleic acid as a consequence of

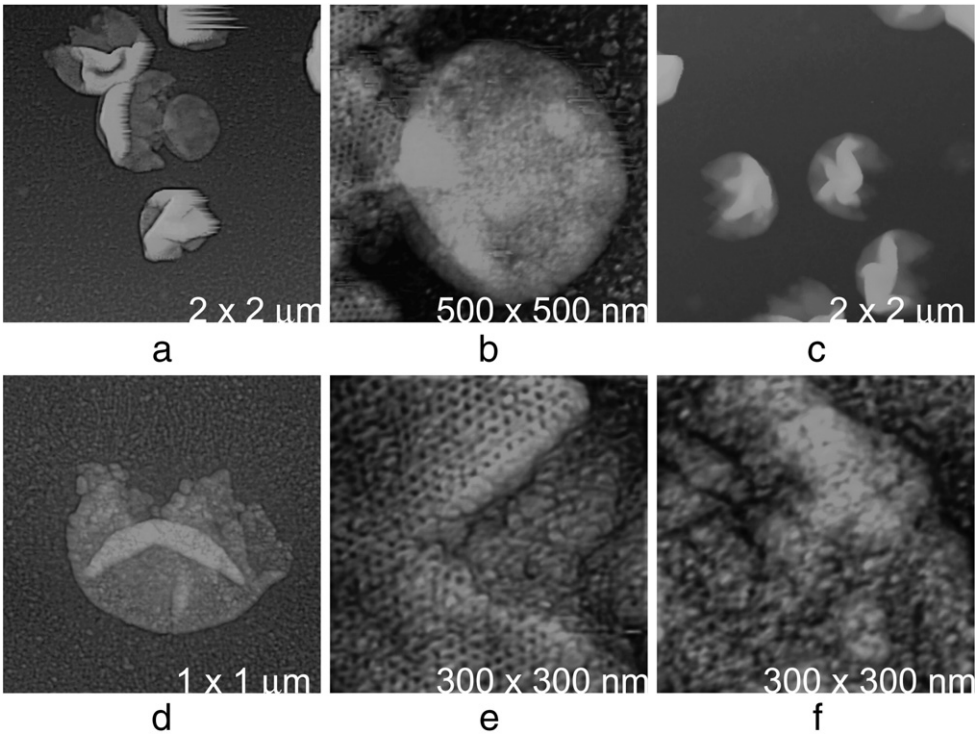

Fig. 7. The AFM image in (a) records a mimivirus capsid expelling the membrane sac containing genomic DNA. In (b) is a higher magnification image of the sac, presumably of lipid bilayer construction, which shows few surface features. The clarity of the icosahedral lattice on the capsid attests, however, to the resolution of the image. Ghosts or capsids that have expelled their DNA containing sacs are also occasionally seen in samples. In (c) and (d) are images that further show how the five triangular faces fold back completely upon emission. These ghosts are additionally useful because they expose the interior surface of the capsids to AFM visualization. In (e) a ghost capsid, having expelled its DNA, has its jaws wide open at the stargate, thereby exposing the inside surface of a "cheek". In (f) is an AFM scan of the inside surface. The interior surface is unlike the outer surface with its regular protein network. It is instead coated with what might be an irregular layer of protein or it may possibly be another lipid membrane.

the enzyme treatments. This was indicated by two observations. First, upon pressing and rupture of particles, only a few, broken virions were observed surrounded by released DNA. The second observation came from particles that were dried on the substrate. While some retained a spherical form upon drying and did contain nucleic acid, a large number deflated and only collapsed shells remained.

In some instances, however, masses of recognizable DNA could be clearly seen bursting from and spreading on the substrate around broken particles. The DNA was always localized about damaged particles and did not appear on the substrate otherwise, eliminating the likelihood of DNA contamination by host DNA. The DNA and its appearance was very similar to the DNA of other viruses that were studied by AFM (Kuznetsov et al., 2005a). The DNA, when spread on the substrate, was not twisted about its self or tightly bundled, but existed as single stands with many turns and loops.

In some experiments, we were successful in forcing the DNA to emerge from a single rupture in a particle, as in Fig. 8c and at higher magnification in (d). The most striking feature of the DNA is that it is highly associated with proteins of various sizes and shapes. Because of the mechanism by which mimivirus delivers its DNA, these proteins would be expected to enter the host cell along with the nucleic acid. We also noted in an earlier investigation (Kuznetsov et al., 2008) that the DNA of vaccinia virus was accompanied, upon its release, by a substantial amount of proteins that varied in sizes, suggesting that a variety of molecules having diverse functionalities were associated with the nucleic acid. With the use of pressure to cause DNA release we could not be certain if the DNA poured from the stargate aperture or through some other portal or wound.

The 7 nm periodicity fibers

On numerous occasions, throughout our investigation of mimivirus, and particularly following disruption of particles, we imaged

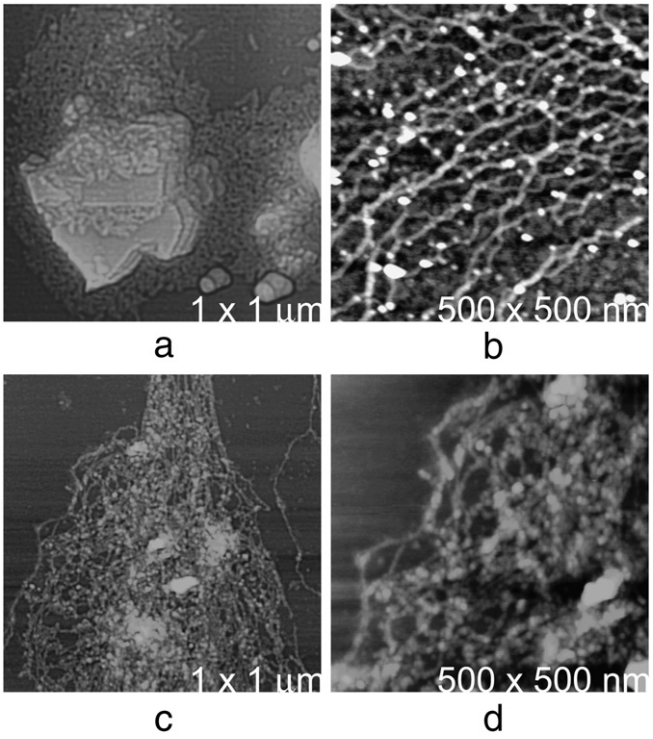

Fig. 8. In (a), a mimivirus has been crushed between plates of cleaved mica and the DNA has burst out of the particle and surrounds the viral remains on the substrate. In (b) is a higher magnification image of some of the DNA strands. In (c) a virion has disgorged its DNA through a single break in the particle onto the substrate. In (d) is a higher magnification image of a tangle of the same DNA, showing it to be heavily associated with protein molecules that exhibit a range of sizes.

fibers that could not be assigned as being either DNA or RNA. We never observed such fibers in studies of other viruses, but we cannot exclude the possibility that they originated from the host amoeba. Thus, presumably these are components of, or associated with mimivirus, the production of virus, or a consequence of host cell infection by mimivirus.

The fibers are very distinctive, sometimes seen as single strands, as in Fig. 9a, but more often organized into cables, bundles, or coils. The fibers, which have a diameter of about 0.9 to 1 nm, display a prominent and easily recognized 7 nm periodicity of dark and light bands. In AFM images dark implies height near the level of the substrate surface while light is an indicator of height above the substrate. Thus a helix, for example, as it rises and falls in a regular manner appears as a periodic sequence of light and dark bands like those exhibited by these fibers.

The periodicity is not due to an AFM artifact, as it is independent of scan direction, and it was observed with many different cantilevers and on many different fibers. The fibers generally tend not to twist or coil about one another, although they do in some cases form cables, but are inclined to associate side by side. Ribbons of fibers thus formed are striking because the fibers do not associate laterally in an arbitrary manner, but in an ordered arrangement so that the 7 nm periodic dark and light bands align between fibers to create many stranded ribbons with 7 nm transverse periodic bands. The fibers and the ribbons they form are quite flexible and, as seen in Fig. 9d for example, can wind into fairly tight coils. Although free ends are sometimes seen in AFM images, most fibers are either of indeterminate length, or at least hundreds of nanometers long. The fibers do not branch. With some exceptions (see below) they do not appear to be associated with other proteins.

In some cases individual 7 nm period fibers are intimately associated with toroidal protein complexes (Fig. 9e and f). The toroidal complexes engage the fibers, with the fibers passing through a rather large, clearly resolved central hole. The assemblies may represent processive enzyme complexes in the act of modifying the fibers. At high magnification, the complexes can be resolved into aggregates of many proteins of varying sizes, and presumably functions.

The 7-nm period fibers of about 1 nm diameter are only infrequently present on the AFM substrate prior to disruption of the virions, but become conspicuous afterwards, hence we have concluded that they are contained within the virions. They are evidently not associated with DNA or emptied from the DNA sac. The only logical place that they could be contained, therefore, is in the space between the interior walls of the icosahedral capsid and the membrane sac containing the DNA. Clearly the fibers cannot be manufactured there, nor are the toroidal protein complexes active in that space. There is simply too little energy and precursor resources available in that volume. Hence we propose that the 7 nm period fibers and their associated toroidal complexes are picked up, acquired from the local milieu (Suzan-Monti et al., 2007) during virion assembly in the previously infected host cell.

Discussion

Fig. 10 contains schematic drawings of a model for the structure of mimivirus based on AFM results, though it is consistent with previous studies using other techniques. To review, most exterior on the virions are globular protein heads of the fibers that first encounter a host cell and insure attachment to its surface. Beneath these are glycosylated fibers that provide a protective layer and are the probable basis for bacterial cell wall mimicry. This dense layer of proteoglycan might perhaps be considered as the beginnings of a primitive cell wall. The base of the fibers is attached to a layer of protein or polypeptide. The surface fibers are likely composed of protein and to be of helical construction. Hence they would be polar, one end suitable for joining to a protein head group, the other end designed to link with anchor polypeptide.

The protein material anchoring the fibers is distributed over the surface of the capsid in a close packed and orderly manner, but with

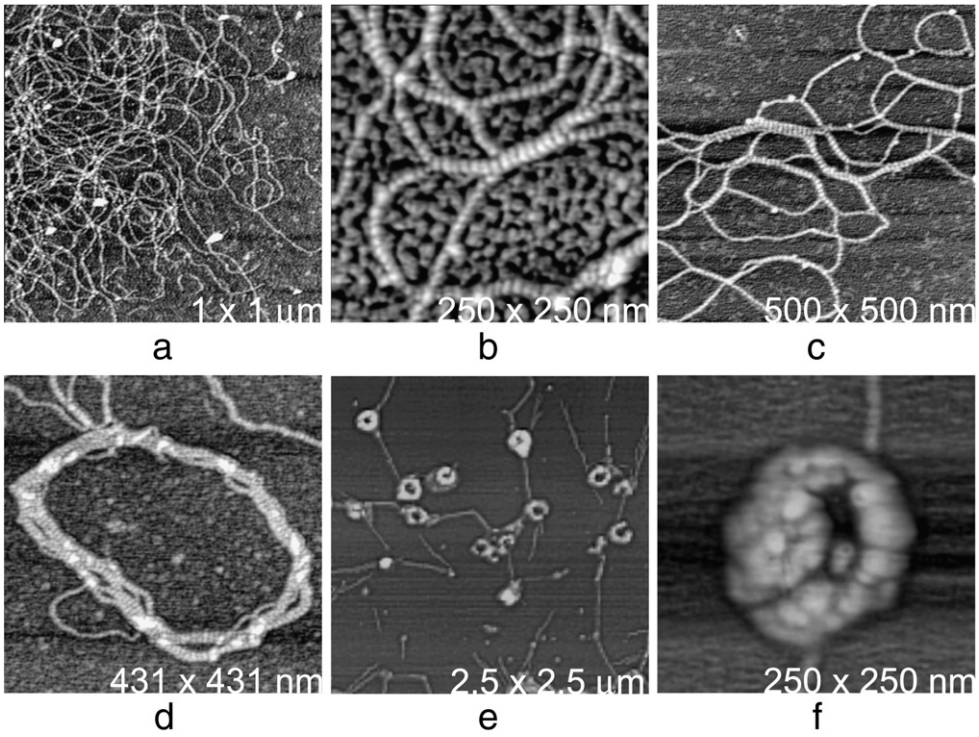

Fig. 9. Partially braided, open networks and coiled superstructures, like those shown in the AFM image of (a) were often observed in close association with disrupted mimivirus. Their distinctive 7 nm light/dark periodicity along their lengths made them easily recognizable. In (b) multiple fibers associate laterally, and in register, to make flat ribbons. In (c) are irregular networks of the fibers and ribbons that commonly form. In (d) a not uncommon coil of ribbons and fibers is recorded. Fibers of 7 nm period are occasionally observed associated with rather large toroidal protein assemblies which may be processive enzyme complexes, as in (e). As is evident in (f), the fibers pass through the center holes of the toroids.

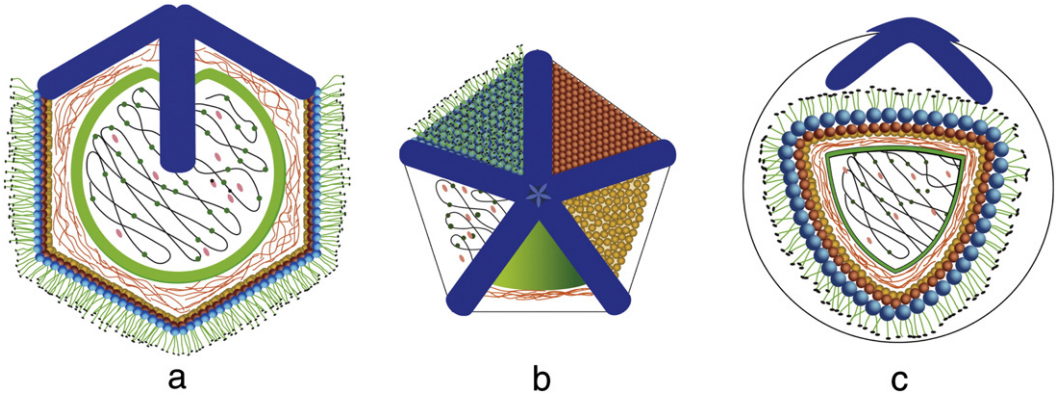

Fig. 10. Schematic drawing of a model for mimivirus viewed in (a) perpendicular to the unique fivefold axis of the particle and in (b) along that axis and into the stargate assembly. In (a) the model is presented in cross section, and in (b) from exterior to interior clockwise as successive layers of structure are revealed. Most exterior (black) are the head proteins of the surface fibers that are attached to the fiber shafts (green). The shafts are attached to the anchor protein, or extended polypeptide loops of MCP (blue spheres) that covers the capsid lattice (red spheres). Beneath the icosahedral capsid is an additional layer (gold) of apparently disorganized protein (or possibly a lipid membrane studded with a variety of proteins). The space between the inner surface of the capsid and the lipid bilayer sac (green) contains the 7 nm fibers of indeterminate length (orange). Inside the membrane is the genomic DNA (black) with associated proteins (green). There are other proteins within the membrane sac that are not directly bound to the nucleic acid and these are in pink. In (c) is a cut-away diagram of mimivirus showing the successive layers of structure using the same color scheme.

no discernable geometric organization. The number of attached fibers is greater than the number of anchor sites, which implies that each anchor is capable of binding multiple fibers. An attractive explanation for this observation, as well as for the honeycomb appearance of degraded particles, is that the anchors are composed of extended, proteolytically susceptible polypeptide loops emerging from the MCP that come together in the lattice depressions. The fact that immature particles, which are along the natural progression to a finished particle, lack fibers but have the anchor layer is consistent with this hypothesis. The loops present multiple sites for attachment, and the bases of the fibers seek and utilize these sites.

Beneath the anchor layer is the capsid composed, in a geometrical sense, of 20 large triangular plates assembled to exhibit icosahedral symmetry (Xiao et al., 2009). The surface lattice is an open, honeycomb arrangement of major capsid protein. Due to proteolysis, cracks appear, principally along icosahedral edges, where strained and probably less stable interactions occur. The edges represent the mechanically weakest structural lines in the capsid, with the junctures between the capsid network and the arms of the stargate excepted.

At a unique vertex of the capsid is the stargate, comprised of five arms that extend from the singular vertex along icosahedral edges. The arms disengage completely from particles and are cast off when the stargate opens. The star assembly is not coated with fibers. The mass of the star apparatus does not lie upon the surface of the capsid, but is enmeshed in the capsid matrix where it forms interactions at seams between the star arms and the honeycomb array of capsid protein. At the center of the star on some particles there appears to be a nascent opening, while on others the center looks to be completely occluded.

When the star opens up, the arms of the star disengage from the particle and the five triangular faces of the capsid, which were in contact with the arms of the star, fold outward. This implies that the capsid shell and the interactions that maintain it possess a substantial degree of plasticity and permit profound structural alterations to occur. The mechanical properties of the capsid and the stargate assembly are quite remarkable, and, as far as we know, unprecedented in viruses. The icosahedral edges were shown to have the mechanical function and properties of hinges.

Once open, a membranous sac containing the DNA emerges from the interior of the capsid. As proposed by Zauberman et al. (2008), *in vivo* this is likely followed either by fusion of the membrane sac with the host cell nuclear membrane and entry of the virus genome as a single mass into the cell nucleus, or fusion with the lysozomal membrane if delivery is to the host cell cytoplasm. The volume of the sac implies a rather loose DNA packing density comparable to what was seen with *vaccinia virus*. There is space inside of the membrane sac to accommodate a significant amount of nucleic acid associated protein as well as the DNA. The membrane-bounded vessel containing the genomic DNA and a complement of essential proteins has many of the characteristics of a proto cell nucleus.

Opening of the stargate also permitted imaging of the inside of the icosahedral capsid by AFM. The inside of the shell is probably coated with yet another layer of protein units of more or less uniform size, but not exhibiting geometric order, or at least discernable geometric order. An alternative possibility is that this layer could be another lipid membrane studded with proteins. A space exists in the capsid interior between the membrane sac and the inside capsid surface amounting to about 30% of the total volume of the capsid.

Spontaneously, or under mechanical stress, DNA was disgorged by some particles. The DNA was, for the most part, unexceptional and had the same general appearance in AFM images as that obtained from other double stranded DNA viruses we have studied (Kuznetsov et al., 2008, 2005a; Kuznetsov and McPherson, 2006). Nucleic acid was not the only class of molecules contained within the membrane sac at the center of a particle. The DNA observed to be pouring out of ruptured virus was associated with many proteins having a range of sizes. These are likely to be enzymes required in at least the early stages of replication and possibly transcription as well (Renesto et al., 2006).

We examined AFM images from hundreds of mimivirus, both intact, untreated virus and degraded particles where the icosahedral capsid was exposed. We could not find any indications on icosahedral faces distal to the star apparatus of an alternative portal or structure that might serve as an entry point for the viral DNA into the capsid. The stargate apparatus appears, from our results, to provide the only aperture for drawing DNA into the capsid and into the membrane sac inside, or for incorporating the membrane sac itself that contains prepackaged DNA. Thus we can lend no support to the proposal of Zauberman et al. (2008) that the DNA enters the capsid through an alternate portal in the center of a triangular face distal to the stargate assembly. On the other hand, Zauberman, et al. described the portal as transient, and that it closed up after DNA entry. Thus no vestigial structure may remain in the mature virion. Rather than being a single strand that is pumped into the capsid (for the same reasons it is not "pumped" into the host), however, it seems equally plausible that the DNA filled sac may enter the capsid by the reverse of its departure, i.e. through the stargate.

The mechanical properties of the icosahedral shell deserve some comment, as they are somewhat unexpected. As noted already, we

suspect that many of the defibered particles in our preparations contained no DNA. For particles lacking DNA, it appears that there was insufficient material to provide internal support to the surrounding icosahedral shell. This is evident when intact particles are dried on the AFM substrate, as in Fig. 11a, or capsids are similarly dried as in Fig. 11b and c. In both cases the particles collapse and the walls of the particles fold upon themselves and form cusp shaped forms.

It is noteworthy that the icosahedral shell does not break or shatter or even crack. It is neither rigid nor brittle, but folds upon itself like a heavy blanket. The icosahedral surface more closely resembles a continuous cloth or textile than an assembly of plates. Thus the individual protein units that compose it, the MCP, must be able to assume a very broad range of conformations or form very flexible interactions with neighbors as the wrinkles and folds are formed over the surface. It is challenging to reconcile such a textured surface structure with the prominent edges, faces, and vertexes of the polygonal shell observed by both electron microscopy, and here by AFM.

It seems quite clear from the AFM images that a capsid assembly pathway by which pre-constructed triangular plates are soldered together at the edges can be eliminated. The capsid is woven as a continuous mesh. The question that remains, however, is what shapes the capsid into its characteristic icosahedral form when it is fully inflated and completely hydrated.

One of the most intriguing observations from our study was of the many very long, flexible fibers, ribbons of fibers, and fiber coils that frequented our AFM images following virus disruption. Lacking other information regarding the fibers, we cannot be certain that they are products of the mimivirus and not material carried over from the host cell during purification. Neither Zauberman et al. (2008) nor Xiao et al. (2009) reported their presence from similar preparations using electron microscopy. There is reason to believe that they did originate from the virus and that they were enclosed in the space between the DNA containing membrane sac and the inside of the capsid. Xiao et al. (2009) note that the DNA containing sac is accurately aligned with the icosahedral capsid, and would thus need support to maintain the icosahedral shape and centrally placed position within the virion. This might be achieved by the fibers.

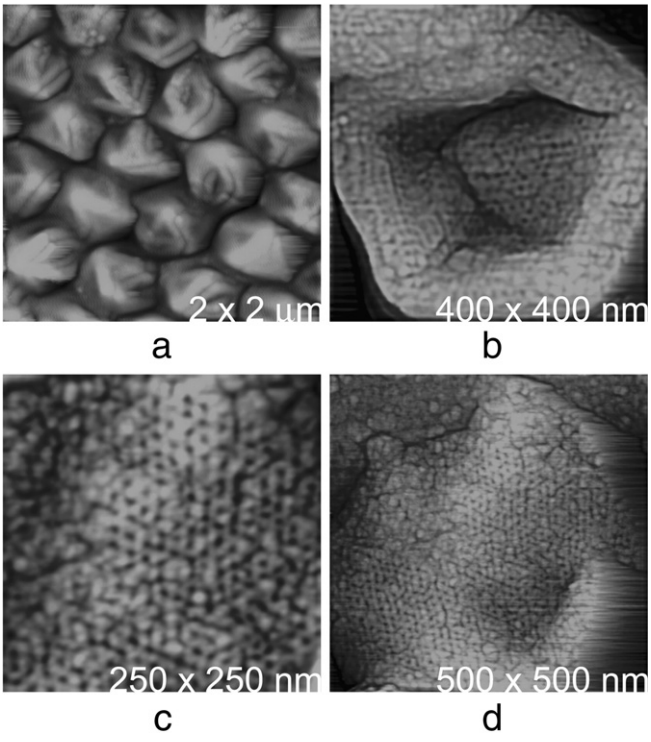

Fig. 11. When mimivirus particles are dried on the AFM substrate, most of the virions collapse like deflated balls, as seen in (a). In (b) a mimivirus capsid obtained by removal of the surface fibers has collapsed as a consequence of drying, assuming a "cup" shape. The icosahedral network of the protein capsid, however, appears intact. This is more evident in (c) which is an image at higher magnification of the surface forming the bottom of the "cup" in (b). In (d) is a large area of a more or less flattened, empty, mimivirus capsid. The protein lattice is still intact and clearly defined, the sheet is virtually undamaged, but the icosahedral properties of the capsid, the vertices, faces, and edges, have become indistinct.

The 1-nm diameter fibers have a striking 7-nm periodicity that is emphasized when the fibers align in register to produce banded ribbons. To our knowledge, there are no polysaccharide or nucleic acid molecules that display such a long repeat, so we assume they must be proteinacious. The small diameter of 1 nm or less, along with their mechanical properties, suggests that the fibers are unlikely to be composed of successive protein subunits joined by non-covalent interactions. Their characteristics appear more consistent with extended protein polymers such as, for example, keratin.

An attractive possibility that we cannot discount is that the long 7-nm period fibers might be precursors of the surface fiber shafts. Indeed, the diameters of the two are quite close, but not identical. In addition, there is no convincing pattern of light and dark bands on the surface fiber shafts. On the other hand, the surface fiber shafts are heavily glycosylated and this might change their apparent diameter as well as obscure an underlying periodicity if it was present.

Another curious observation contained in the AFM images is that single strands of the 7-nm periodic fibers are occasionally associated with toroidal complexes, which we feel are likely to be processive enzyme complexes of some sort (Breyer and Matthews, 2001). The toroids have a break, or cut in their circumference that would permit them to slip around a fiber and then move along it. The fibers were seen to pass through the hole in the centers of the toroids. The images apparently captured the toroidal complexes, which are composed of a number of protein subunits of varying sizes, in the act of modifying the fibers.

Mimivirus may be an extraordinarily complex and advanced virus, or a sadly degenerate cell, but these structural studies indicate, as did others before, that it shares the properties of both. Thus its origin remains a puzzle. It seems certain, in any case, that more layers of complexity will emerge with further studies of the mimivirus architecture and life cycle that will clarify its co-evolution in conjunction with its hosts, or its separate evolution from an earlier, more primitive pre-biological molecular assembly. The structural model presented here serves only as a starting point to be further shaped and detailed by future studies.

Materials and methods

Virus propagation and purification

Acanthamoeba polyphaga were grown to confluence, infected with Mimivirus and incubated at 32 °C. Upon completion of infection, the culture was filtered through a 0.8 micron filter to remove amoeba debris. The filtrate was then centrifuged at 10,000*g* for 10 min. The mimivirus pellet was washed with PBS buffer twice and resuspended in PBS buffer.

Digestion of virus

Mimivirus fibers were digested by sequential application of lysozyme and bromelain. Following collection by centrifugation at 1000*g* for 30 min, each volume of pelleted virus was incubated with four volumes of 10 mg/ml lysozyme in TES buffer (0.05 M N-[Tris(hydroxymethyl) methyl]-2-aminoethanesulfonic acid, pH 7.5, 0.01% NaN3) at room temperature at least 1 day. The samples were washed twice with TES and digested with five volumes of 14 mg/ml bromelain from pineapple stem (Sigma) in TES buffer (0.035 M TES, pH 7.5, 0.3 M KCl, 0.02 M DTT), at room temperature, for at least 1 day. Virus particles that were treated

with lysozyme and bromelain, were, in some experiments, further exposed to 1 mg/ml solutions of proteinase K and 1% SDS at 37 °C for 30 min to 2 h, washed with distilled water, and then imaged by AFM.

AFM analysis

For experiments where the virus was treated *in vitro* and then visualized by AFM, samples of virus, or virions treated with specific reagents were spread on poly-L-lysine coated slips of cleaved mica and fixed by *in situ* exposure for 15 min to 5% glutaraldehyde. The substrates were then either dried in air and imaged, or washed two to three times with water before analysis. For AFM imaging in air the sample was dried in a stream of nitrogen gas before imaging.

Fixation with glutaraldehyde has been shown in previous studies not, to the resolution of the AFM technique, to perturb the surface structure of viral particles, and poly-L-lysine insures adherence of virus particles and their components to the substrate (Kuznetsov et al., 2002; 2005a; 2004; 2001; 2003).

AFM analysis was carried out using a Nanoscope III multimode instrument (Veeco Instruments, Santa Barbara, CA). Imaging procedures were fundamentally the same as described for previous investigations of viruses (Kuznetsov et al., 2002; 2001; 2003); and RNA (Kuznetsov et al., 2005b; Kuznetsov and McPherson, 2006). Hydrated samples were scanned at 26 °C using oxide-sharpened silicon nitride tips in a 75-μl fluid cell containing buffer. For scanning in air, silicon tips were employed. The images were collected in tapping mode (Hansma and Hoh, 1994; Hansma and Pietrasanta, 1998) with an oscillation frequency of 9.2 kHz in fluid and 300 kH in air, with a scan frequency of 1 Hz.

In the AFM images presented here, height above substrate is indicated by increasingly lighter color. Thus points very close to the substrate are dark and those well above the substrate white. Because lateral distances are distorted due to an AFM image being the convolution of the cantilever tip shape with the surface features scanned, quantitative measures of size were based either on heights above the substrate, or on center to center distances on particle surfaces. The AFM instrument was calibrated to the small lateral distances by imaging the 111 face of a thaumatin protein crystal and using the known lattice spacing (Ko et al., 1994; Kuznetsov et al., 1999) as standard.

Acknowledgments

We thank Susan Hafenstein for her earlier participation in this work as well as Rodney McPhael for help in producing Fig. 10 and Aaron Greenwood for preparation of all other figures. The work was supported by NIH grant AI11219 to MGR.

References

Benson, S.D., Bamford, J.K., Bamford, D.H., Burnett, R.M., 2004. Does common architecture reveal a viral lineage spanning all three domains of life? Mol. Cell 16 (5), 673–685.
Breyer, W.A., Matthews, B.W., 2001. A structural basis for processivity. Protein Sci. 10 (9), 1699–1711.
Casjens, S., Ed. (1997). Principles of Virion Structure, Function, and Assembly. Structural Biology of Viruses. Edited by W. Chu, R. M. Burnett, and R. Garcia. Oxford: Oxford Univ. Press.
Casjens, S., Weigele, P., 2005. Headful DNA packaging by bacteriophage P22. In: Calalano, C. (Ed.), Viral genome packaging machines. Genetics, structure and mechanisms. Landis Publishing, Georgetown, TX, pp. 80–88.
Claverie, J.M., Ogata, H., Audic, S., Abergel, C., Suhre, K., Fournier, P.E., 2006. Mimivirus and the emerging concept of "giant" virus. Virus Res. 117 (1), 133–144.
Claverie, J.M., Abergel, C., Ogata, H., 2009. Mimivirus. Curr. Top. Microbiol. Immunol. 328, 89–121.
Forterre, P., 2006. The origin of viruses and their possible roles in major evolutionary transitions. Virus Res. 117 (1), 5–16.
Hansma, H.G., Hoh, J.H., 1994. Biomolecular imaging with the atomic force microscope. Annu. Rev. Biophys. Biomol. Struct. 23, 115–139.
Hansma, H.G., Pietrasanta, L., 1998. Atomic force microscopy and other scanning probe microscopies. Curr. Opin. Chem. Biol. 2 (5), 579–584.
Kindt, J., Tzlil, S., Ben-Shaul, A., Gelbart, W.M., 2001. DNA packaging and ejection forces in bacteriophage. Proc. Natl. Acad. Sci. U. S. A. 98 (24), 13671–13674.
Ko, T.P., Day, J., Greenwood, A., McPherson, A., 1994. Structures of three crystal forms of the sweet protein thaumatin. Acta Crystallogr. D Biol. Crystallogr. 50 (Pt 6), 813–825.
Kuznetsov, Y.G., McPherson, A., 2006. Identification of DNA and RNA from retroviruses using ribonuclease A. Scanning 28 (5), 278–281.
Kuznetsov, Y.G., Konnert, J., Malkin, A.J., McPherson, A., 1999. The advancement and structure of growth steps on thaumatin crystals visualized by atomic force microscopy at molecular resolution. Surf. Sci. 440, 69–80.
Kuznetsov, Y.G., Malkin, A.J., Lucas, R.W., Plomp, M., McPherson, A., 2001. Imaging of viruses by atomic force microscopy. J. Gen. Virol. 82 (Pt 9), 2025–2034.
Kuznetsov, Y.G., Datta, S., Kothari, N.H., Greenwood, A., Fan, H., McPherson, A., 2002. Atomic force microscopy investigation of fibroblasts infected with wild-type and mutant murine leukemia virus (MuLV). Biophys. J. 83 (6), 3665–3674.
Kuznetsov, Y.G., Victoria, J.G., Robinson Jr., W.E., McPherson, A., 2003. Atomic force microscopy investigation of human immunodeficiency virus (HIV) and HIV-infected lymphocytes. J. Virol. 77 (22), 11896–11909.
Kuznetsov, Y.G., Low, A., Fan, H.Y., McPherson, A., 2004. Atomic force microscopy investigation of wild type moloney murine leukemia virus particles and virus particles lacking the envelope protein. Virology 323, 189–196.
Kuznetsov, Y.G., Gurnon, J.R., Van Etten, J.L., McPherson, A., 2005a. Atomic force microscopy investigation of a chlorella virus, PBCV-1. J. Struct. Biol. 149 (3), 256–263.Kuznetsov, Y.G., Low, A., Fan, H., McPherson, A., 2005a. Atomic force microscopy investigation of isolated virions of murine leukemia virus. J. Virol. 79 (3), 1970–1974.
Kuznetsov, Y.G., Daijogo, S., Zhou, J., Semler, B.L., McPherson, A., 2005b. Atomic force microscopy analysis of icosahedral virus RNA. J. Mol. Biol. 347 (1), 41–52. Kuznetsov, Y.G., Zhang, M., Menees, T.M., McPherson, A., Sandmeyer, S., 2005b. Investigation by atomic force microscopy of the structure of Ty3 retrotransposon particles. J. Virol. 79 (13), 8032–8045.
Kuznetsov, Y.G., Ulbrich, P., Haubova, S., Ruml, T., McPherson, A., 2007. Atomic force microscopy investigation of Mason-Pfizer monkey virus and human immunodeficiency virus type 1 reassembled particles. Virology 360 (2), 434–446.
Kuznetsov, Y., Gershon, P.D., McPherson, A., 2008. Atomic force microscopy investigation of vaccinia virus structure. J. Virol. 85, 7551–7566.
Lucas, R.W., Kuznetsov, Y.G., Larson, S.B., McPherson, A., 2001. Crystallization of Brome Mosaic Virus (BMV) and T = 1 Brome Mosaic Virus Particles following a structural transition. Virology 286, 290–303.
Lyer, L.M., Aravind, L., Koonin, E.V., 2001. Common origin of four diverse families of large eukaryotic DNA viruses. J. Virol. 75 (23), 11720–11734.
McPherson, A., 1999. Crystallization of biological macromolecules. Cold Spring Harbor Laboratory Press, Cold Spring Harbor, NY.
Moreira, D., Lopez-Garcia, P., 2009. Ten reasons to exclude viruses from the tree of life. Nat. Rev. Microbiol. 7 (4), 306–311.
Raoult, D., Forterre, P., 2008. Redefining viruses: lessons from Mimivirus. Nat. Rev. Microbiol. 6 (4), 315–319.
Raoult, D., Audic, S., Robert, C., Abergel, C., Renesto, P., Ogata, H., La Scola, B., Suzan, M., Claverie, J.M., 2004. The 1.2-megabase genome sequence of Mimivirus. Science 306 (5700), 1344–1350.
Raoult, D., La Scola, B., Birtles, R., 2007. The discovery and characterization of Mimivirus, the largest known virus and putative pneumonia agent. Clin. Infect. Dis. 45 (1), 95–102.
Renesto, P., Abergel, C., Decloquement, P., Moinier, D., Azza, S., Ogata, H., Fourquet, P., Gorvel, J.P., Claverie, J.M., 2006. Mimivirus giant particles incorporate a large fraction of anonymous and unique gene products. J. Virol. 80 (23), 11678–11685.
Suzan-Monti, M., La Scola, B., Raoult, D., 2006. Genomic and evolutionary aspects of Mimivirus. Virus Res. 117 (1), 145–155.
Suzan-Monti, M., La Scalo, B., Barrassi, L., Espinosa, L., Raoult, D., 2007. Ultrastructural characterization of the giant volcano - like virus factory of Acanthamoeba polyphaga mimivirus. PLoS ONE 2 (3), e328.
Van Etten, J.L., Lane, L.C., Meints, R.H., 1991. Viruses and virus like particles of eukaryotic algae. Microbiol. Rev. 55, 586–620.
Xiao, C., Chipman, P.R., Battisti, A.J., Bowman, V.D., Renesto, P., Raoult, D., Rossmann, M.G., 2005. Cryo-electron microscopy of the giant Mimivirus. J. Mol. Biol. 353 (3), 493–496.
Xiao, C., Kuznetsov, Y.G., Sun, S., Hafenstein, S.L., Kostyuchenko, V.A., Chipman, P.R., Suzan-Monti, M., Raoult, D., McPherson, A., Rossmann, M.G., 2009. Structural studies of the giant mimivirus. PLoS Biol. 7 (4), 958–966.
Yamada, T., Onimatsu, H., Van Etten, J.L., 2006. Chlorella viruses. Adv. Virus Res. 66, 293–336.
Zauberman, N., Mutsafi, Y., Halevy, D.B., Shimoni, E., Klein, E., Xiao, C., Sun, S., Minsky, A., 2008. Distinct DNA exit and packaging portals in the virus *Acanthamoeba polyphaga* mimivirus. PLoS Biol. 6 (5), e114.